JOURNAL OF APPLIED ELECTROCHEMISTRY 24 (1994) 44–51

Effect of gelling on the open circuit potential against time transients of $Pb/PbSO_4$ electrodes at various states of charge*

M. P. VINOD, K. VIJAYAMOHANAN‡

Materials Chemistry Division, National Chemical Laboratory, Pune-411008, India

Received 27 April 1993; revised 19 July 1993

The technique of open-circuit potential relaxation from a prior prepolarized state has been employed to study the kinetics of the $Pb/PbSO_4$ electrode in 4.8 M sulphuric acid. The significant features governing the relaxation have been quantitatively analysed to obtain a correlation between state-of-charge of the electrode and its potential–recovery time constant. The effect of immobilizing the electrolyte has also been included due to its relevance in making sealed maintenance-free batteries. The study provides a method for estimating the variation of exchange current density of the $Pb/PbSO_4$ and hydrogen evolution reactions at various states-of-charge with and without added gelling agents.

1. Introduction

Measurement and analysis of the relaxation of open-circuit potential provides useful information regarding the interfacial characteristics of electrochemical reactions [1–6]. Specifically, this includes capacitance behaviour of the electrode–solution interface [3–7], kinetic and mechanistic behaviour of the electrode reactions [8–10] and potential-dependent adsorption pseudo-capacitance associated with the coverage variation of chemisorbed species etc. This technique is especially important when steady state measurements are difficult due to the time dependence of overpotential or the variation of coverage by adsorbed species with potential and time. This difficulty is often realized in several experimental systems such as corroding battery electrodes, other film-covered interfaces and electrodes with attached gas bubbles.

The open-circuit potential (o.c.p.) relaxation technique has been employed successfully for the past two decades for various battery electrodes such as PbO_2 [8], NiOOH [6, 7, 9], Mg [10], Fe [11] and Zn [12]. A similar understanding of the mechanism governing the transients of the $Pb/PbSO_4$ electrode in sulphuric acid electrolyte is both of theoretical and practical interest. Although the technique of the o.c.p.–time transient has been employed for the $Pb/PbSO_4$ electrode in sulphuric acid by Pavlov [13], the objective was to analyse the mechanism of passivation along with the alkalisation of solution in the pores subsequent to the formation of PbO and basic $PbSO_4$. The transients were found to be governed by processes associated with the disappearance of alkalization in the pores. A fundamental analysis of electrode kinetics of the $Pb/PbSO_4$ system was not attempted.

As the modern trend to develop sealed maintenance-free lead–acid batteries with gelled or adsorbed electrolytes continues, it is of practical importance to analyse the effect of gelling on the electrode kinetics of the $Pb/PbSO_4$ electrode. Furthermore, this analysis of o.c.p. decay with or without gel can provide a correlation between the parameters of self-discharge kinetics and the observed potential–recovery time constants. The latter aspect will be useful for improving the shelf life of maintenance-free batteries and also in designing cells for special purposes like pulsed discharge [14, 15].

In this work an analysis of the open-circuit potential–time transients of $Pb/PbSO_4$ electrodes was attempted at various states-of-charge (s.o.c.); the effect of immobilizing the electrolyte using sodium silicate gel on the kinetics of $Pb/PbSO_4$ electrode was also investigated. In addition, the study provides a means to estimate self discharge rate from the slope of such o.c.p.–time transients.

2. Experimental details

Positive and negative lead-acid plates were obtained in cured and formed condition from the production line at UB-MEC Batteries Ltd, India. All the electrodes were made using the same grid materials namely, with Pb–Ca(0.08%)–Sn(0.5%), to exclude possible effects of interaction by corrosion products. Negative limited test cells with excess sulphuric acid (4.8 M) electrolyte were assembled with two positive counter electrodes arranged on either side of the working electrode.

* This paper is dedicated to the memory of the late Professor S. Sathyanarayana.

‡ To whom all correspondence should be addressed.

0021-891X

The potential of the working electrode was measured against a Hg/Hg_2SO_4, H_2SO_4 (4.8 M) reference electrode. The reference electrode was connected to the test cell with a capillary bridge filled with sulphuric acid (4.8 M) and provided with a closed ungreased stopcock. The bridge terminated in a luggin type capillary tip aligned close to the centre of the working electrode. All potentials are reported relative to this reference electrode. The electrode potentials were measured, correct to +0.1 mV, by connecting a buffer amplifier with unit gain and substantially high input impedance ($10^{13}\ \Omega$) between the working and reference electrodes [16].

The electrodes were given an initial soaking of 10 h in 4.8 M sulphuric acid and then the cell was subsequently subjected to galvanostatic charging and discharging ($C/10$ rate) for five cycles to stabilize the capacity. The discharge and charge cutoff points for these cycles were −0.85 and −1.2 V, respectively. The s.o.c. was calculated on the basis of the stabilized capacity at the end of the fifth cycle. At the end of the sixth charge, the cells were then given the same amount of overcharge (20%), kept at o.c.p. for 30 min and then discharged at the $C/10$ rate. At the end of discharge potential–time data were collected at room temperature (25 ± 1° C). The experiments were repeated at each s.o.c. values with immobilized electrolyte prepared by using sodium silicate (5 g dm^{-3}) as the gelling agent [17].

3. Results and discussion

Figures 1 and 2 show data for the o.c.p. recovery of the $Pb/PbSO_4$ electrode following the interruption of a prior anodic polarization in ungelled and gelled electrolyte, respectively, at various state-of-charge (s.o.c.) values. The instantaneous variation in the electrode potential caused by the ohmic drop makes the transient very steep at the onset. This recovery appears to be faster in the case of ungelled electrolyte at all s.o.c. values. Subsequent to this initial steep drop the potential varies slowly with time, approaching the equilibrium values asymptotically. The physicochemical processes governing this relaxation are independent of s.o.c. as the attainment of equilibrium is fairly fast and is complete within 15 s. This is in contrast to the PbO_2 electrode in which the relaxation time constant, as well as the equilibrium potential varies with s.o.c. [8]. Moreover, the variation over longer times is much faster for the case with immobilized electrolyte, indicating the increased hindrance to mass transfer. This is more pronounced at lower s.o.c. values. For example, in the case of ungelled electrolyte 95% of the relaxation is complete within 20 s, even at an s.o.c. of 0.05, but requires several minutes for the gelled electrolyte case.

Figures 3 and 4 show the o.c.p.–time transients for the ungelled and gelled electrolytes subsequent to the interruption of the cathodic current. The main features are simlar to those for the anodic case, suggesting that a similar reaction, the reduction of $PbSO_4$ to Pb, controls the relaxation kinetics. However, in the case of all s.o.c. values, except perhaps the case of the lowest one (0.2), the possibility of simultaneous hydrogen evolution and $PbSO_4$ reduction contributing to the relaxation is more likely. Although these transient patterns progressively change with s.o.c. the immobilization has very little effect at high s.o.c. values on the cathodic recovery curves, unlike the cases represented in Figs 1 and 2.

3.1. *Theoretical analysis of o.c.p. transients*

Several electrochemical reactions can possibly occur on a $Pb/PbSO_4$ electrode under open-circuit conditions [18]. Among these the important potential-determining reactions are as follow:

$$PbSO_4 + 2e^- \longrightarrow Pb + SO_4^{2-} \quad E^0 = -0.9716 \quad (1)$$

$$2H^+ + 2e^- \longrightarrow H_2 \quad E^0 = -0.6186 \quad (2)$$

$$O_2 + 4H^+ + 4e^- \longrightarrow 2H_2O \quad E^0 = 0.6116 \quad (3)$$

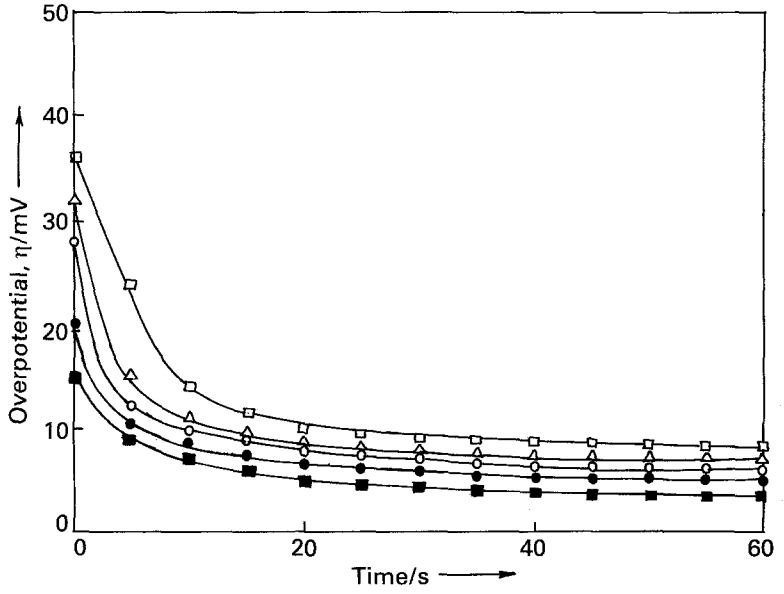

Fig. 1. Open-circuit potential–time transients following the interruption of a prior anodic polarization of the $Pb/PbSO_4$ electrode in 4.8 M sulphuric acid at various s.o.c. values: (■) 0.995, (●) 0.8, (○) 0.5, (△) 0.2 and (□) 0.05.

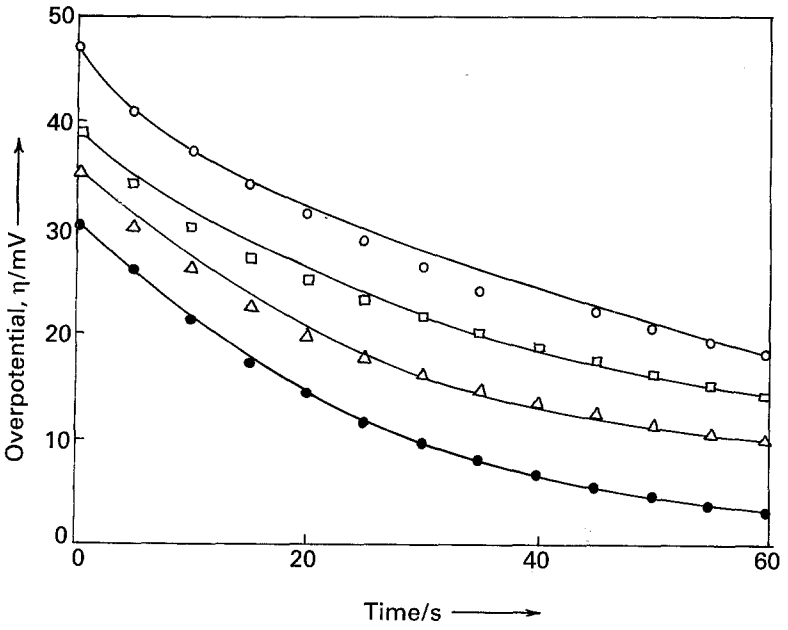

Fig. 2. Open-circuit potential–time transients following the interruption of a prior anodic polarization of the $Pb/PbSO_4$ electrode in 4.8 M gelled sulphuric acid at various s.o.c. values: (●) 0.8, (△) 0.5, (□) 0.2 and (○) 0.05.

The $Pb/PbSO_4$, H_2SO_4 electrode under open-circuit is in a steady state when current flows between the $Pb/PbSO_4$ and $\frac{1}{2}H_2/H^+$ electrodes. That is, the observed potential is a corrosion potential (mixed potential) having a contribution from anodic lead dissolution and cathodic hydrogen evolution. This is especially significant at higher s.o.c. values, where the concentration of $PbSO_4$ is small compared to that of lead. The potential relaxation from a steady state value during polarization to such a mixed potential following the interruption of the current in a galvanostatic mode can be expressed by the mutual compensation of faradaic and nonfaradaic currents. That is

$$-C(\mathrm{d}\eta/\mathrm{d}t) + \sum I_{\text{faradaic}} = 0 \qquad (4)$$

where C is the double layer capacity, I_{faradaic} is the potential dependent current for various faradaic processes such as Reactions 1, 2 and 3 and η is the overpotential undergoing relaxation. The value of η also determines the magnitude of the open-circuit self discharge current. The resistance polarization can be considered to be absent as the net current is zero. Under these circumstances the relaxation of the o.c.p. following current interruption can be analysed with the help of electrochemical Reactions 1, 2 and 3 by using Equation 4.

$$\begin{aligned} -C(\mathrm{d}\eta/\mathrm{d}t) + I_{0,\mathrm{Pb}}[\exp(-\alpha_{\mathrm{Pb}} f\eta_{\mathrm{Pb}}) - \exp(\beta_{\mathrm{Pb}} f\eta_{\mathrm{Pb}})] \\ + I_{0,\mathrm{H}}[\exp(-\alpha_{\mathrm{H}} f\eta_{\mathrm{H}}) - \exp(\beta_{\mathrm{H}} f\eta_{\mathrm{H}})] \\ + I_{0,\mathrm{O}}[\exp(-\alpha_{\mathrm{O}} f\eta_{\mathrm{O}}) - \exp(\beta_{\mathrm{O}} f\eta_{\mathrm{O}})] = 0 \end{aligned} \qquad (5)$$

where $I_{0,\mathrm{Pb}}$, $I_{0,\mathrm{H}}$ and $I_{0,\mathrm{O}}$ are the exchange currents for Reactions 1, 2 and 3, respectively. Similarly α and β are the apparent cathodic and anodic energy transfer coefficients; η_{Pb}, η_{H} and η_{O} are the overpotentials defined as $E - E^{\mathrm{r}}_{\mathrm{Pb}}$, $E - E^{\mathrm{r}}_{\mathrm{H}}$ and $E - E^{\mathrm{r}}_{\mathrm{O}}$, respectively and f is defined as nF/RT where n is the number of electrons involved in the respective reactions and F, R and T have their usual significance.

Equation 5 is valid only if mass transfer polarization is negligible for all the faradaic reactions. A high concentration of sulphuric acid (4.8 M)

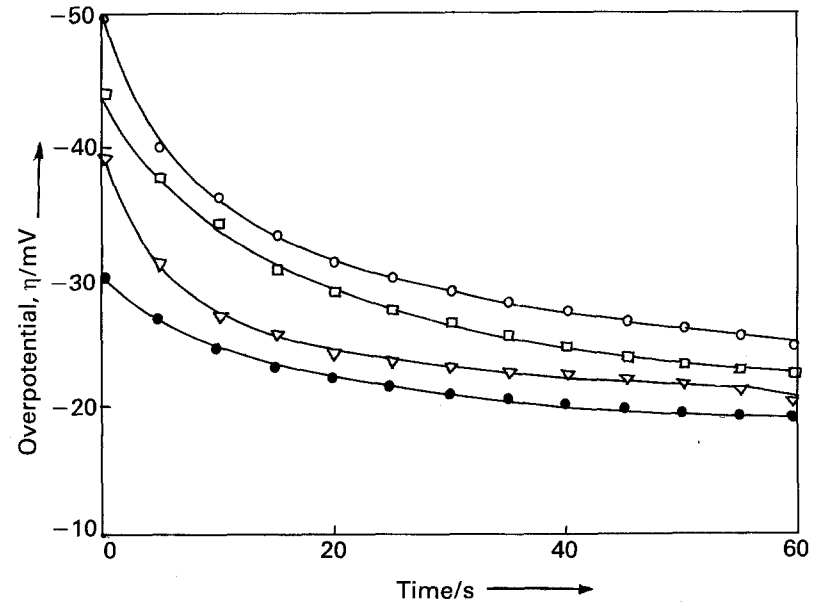

Fig. 3. Open-circuit potential–time transients following the interruption of a prior cathodic polarization of the $Pb/PbSO_4$ electrode in 4.8 M sulphuric acid at various s.o.c. values: (□) 1, (△) 0.8, (○) 0.5 and (●) 0.2.

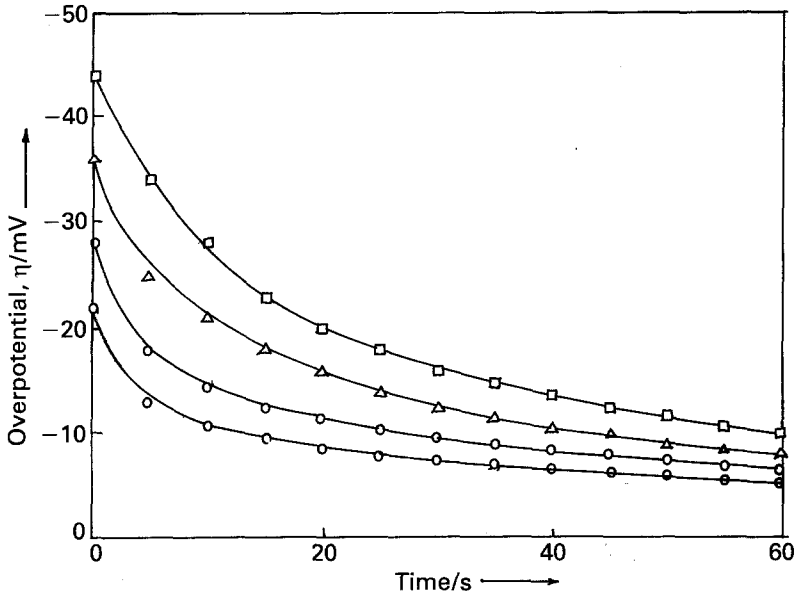

Fig. 4. Open-circuit potential–time transients following the interruption of a prior cathodic polarization of the Pb/$PbSO_4$ electrode in 4.8 M gelled sulphuric acid at various s.o.c. values: (○) 1, (□) 0.8, (▽) 0.5 and (●) 0.2.

employed in the experiment and invariance of the observed o.c.p. decay patterns with stirring suggest the absence of mass transfer control.

As a first approximation, one may avoid the third term in Equation 5 because of kinetic reasons*. Oxygen mass transfer is a relatively slow process; in addition, the electrolyte is likely to be saturated with hydrogen initially at least at high s.o.c. values, due to corrosion of the lead electrodes. Hence, the oxygen reduction may be neglected and Equation 5 becomes

$$-C(\mathrm{d}\eta/\mathrm{d}t) + I_{0,\mathrm{Pb}}[\exp(-\alpha_{\mathrm{Pb}}f\eta_{\mathrm{Pb}}) - \exp(\beta_{\mathrm{Pb}}f\eta_{\mathrm{Pb}})] + I_{0,\mathrm{H}}[\exp(-\alpha_{\mathrm{H}}f\eta_{\mathrm{H}}) - \exp(\beta_{\mathrm{H}}f\eta_{\mathrm{H}})] = 0 \quad (6)$$

An examination of the observed o.c.p.–time transients indicates that the hydrogen evolution reaction is in the Tafel domain in the potential ranges under consideration [$\eta_{\mathrm{H}} \gg RT/nF$], hence the above equation can be modified to

$$-C(\mathrm{d}\eta/\mathrm{d}t) + I_{0,\mathrm{Pb}}[\exp(-\alpha_{\mathrm{Pb}}f\eta_{\mathrm{Pb}}) - \exp(\beta_{\mathrm{Pb}}f\eta_{\mathrm{Pb}})] + I_{0,\mathrm{H}}[\exp(-\alpha_{\mathrm{H}}f\eta_{\mathrm{H}})] = 0 \quad (7)$$

This expression is the governing equation for o.c.p. transients of the Pb/$PbSO_4$ electrode in sulphuric acid at various s.o.c. values. It includes the charge transfer polarization of the reversible Pb/$PbSO_4$ system and the irreversible cathodic hydrogen evolution reaction (h.e.r.), compensated by the nonfaradaic component expressed by the first term. This expression can be used for the analysis of o.c.p.–time transients subsequent to cathodic as well as anodic interruption as follows.

During the relaxation from a prior anodic polarization the lead electrode (unless its s.o.c. is near zero) attains a mixed or corrosion potential, E_{cor}, with lead dissolution occurring with hydrogen evolution. The measured potential approaches E_{cor} as ($\mathrm{d}\eta/\mathrm{d}t$) approaches zero. At high s.o.c. values as little $PbSO_4$ is present in the electrode, the $PbSO_4$ reduction can be neglected in comparison with dissolution of lead during the relaxation from anodic polarization. Hence Equation 7 becomes

$$-C(\mathrm{d}\eta/\mathrm{d}t) - I_{0,\mathrm{Pb}}[\exp)\beta_{\mathrm{Pb}}f\eta_{\mathrm{Pb}})] + I_{0,\mathrm{H}}[\exp(-\alpha_{\mathrm{H}}f\eta_{\mathrm{H}})] = 0 \quad (8)$$

and, consequently, the corrosion current is

$$I_{\mathrm{cor}} = I_{0,\mathrm{Pb}}[\exp(\beta_{\mathrm{Pb}}f(E^{\mathrm{cor}} - E^{\mathrm{r}}_{\mathrm{Pb}})] = I_{0,\mathrm{H}}[\exp(-\alpha_{\mathrm{H}}f(E^{\mathrm{cor}} - E^{\mathrm{r}}_{\mathrm{H}})] \quad (9)$$

where the overpotential for the lead dissolution and hydrogen evolution are substituted by the respective shift from their reversible values.

Substituting $I_{0,\mathrm{Pb}}$ and $I_{0,\mathrm{H}}$ into Equation 8 and simplifying

$$-C(\mathrm{d}\eta/\mathrm{d}t) - I_{\mathrm{cor}}\{\exp[\beta_{\mathrm{Pb}}f(E - E_{\mathrm{cor}})]\} + I_{\mathrm{cor}}\{\exp[-\alpha_{\mathrm{H}}f(E - E_{\mathrm{cor}})]\} = 0 \quad (10)$$

In the potential domain where $|E - E_{\mathrm{cor}}| \ll 1/f$ Equation 10 can be linearized to obtain

$$(\mathrm{d}\eta/\mathrm{d}t) = -[I_{\mathrm{cor}}(\alpha_{\mathrm{H}} + \beta_{\mathrm{Pb}})f/C]E + [I_{\mathrm{cor}}(\alpha_{\mathrm{H}} + \beta_{\mathrm{Pb}})f/C]E_{\mathrm{cor}} = 0 \quad (11)$$

Thus a plot of ($\mathrm{d}\eta/\mathrm{d}t$) against E will be straight line with a slope of $I_{\mathrm{cor}}f(\alpha_{\mathrm{H}} + \beta_{\mathrm{Pb}})/C$. Furthermore, this slope and intercept can be used to calculate the double layer capacitance and corrosion current with a prior knowledge of α_{H} and β_{Pb} values.

For the case of lower s.o.c. values, although the h.e.r. is thermodynamically possible, the presence of a large amount of $PbSO_4$ demands Pb^{2+} reduction as the major potential determining reaction. This is further supported by the fact that exchange currents are much larger for Pb^{2+} reduction in comparison with that for h.e.r., i.e. $i_{0,\mathrm{Pb}}/i_{0,\mathrm{H}} > 10^3$ [19]. Also, experimentally, the h.e.r. is not observed during the decay except perhaps at s.o.c. equal to unity. Under these circumstances Equation 7 can be

* Although the possibility of oxygen reduction cannot be strictly ruled out in a maintenance-free battery with glass fibre separator or in a stirred cell with oxygen evolution from PbO_2 electrodes its relative contribution is negligible as $I_{0,\mathrm{Pb}}/I_{0,\mathrm{O}} \geqslant 10^4$ [19].

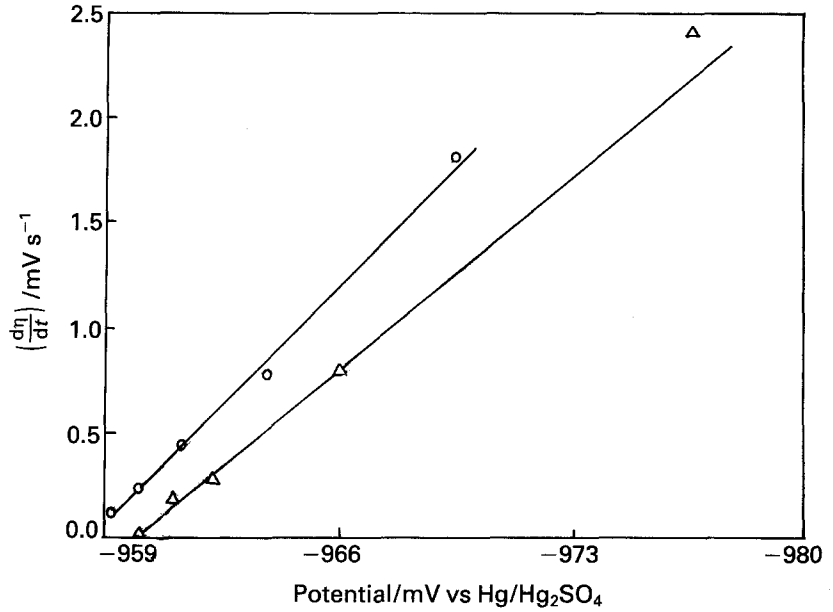

Fig. 5. ($d\eta/dt$) against E plots using the data from Fig. 1 at various s.o.c. values: (○) 0.995 and (△) 0.8.

written as

$$-C(d\eta/dt) + I_{0,Pb}[\exp(-\alpha_{Pb} f \eta_{Pb})] - I_{0,Pb}[\exp(\beta_{Pb} f \eta_{Pb})] = 0 \quad (12)$$

Assuming $\alpha_{Pb} = \beta_{Pb} = \alpha$ the above expression can be written as

$$-C(d\eta/dt) + 2I_{0,Pb} \sinh(\alpha f \eta_{Pb}) = 0 \quad (13)$$

The solution of this differential equation is

$$\ln[\tanh(\alpha f \eta_{Pb}/2)] = -(2I_{0,Pb} f/C)t + \text{constant} \quad (14)$$

Hence by plotting $\ln[\tanh(\alpha f \eta_{Pb}/2)]$ against t, the exchange current density for the $Pb/PbSO_4$ system can be calculated from the slope. Furthermore, any change in the slope due to immobilization can be attributed to the variation of $I_{0,Pb}$, assuming that C does not vary appreciably with immobilization.

Alternatively, if η is very small compared to $1/\alpha f$ Equation 12 can be linearized to obtain

$$-C(d\eta/dt) - I_{0,Pb} f \eta_{Pb} = 0 \quad (15)$$

with the additional assumption ($\alpha_{Pb} + \beta_{Pb}$) equal to unity. This gives,

$$\ln \eta = -(I_{0,Pb} f)/C \times t + \text{constant} \quad (16)$$

Hence a plot of $\ln \eta$ against t will be straight line with a slope of $-I_{0,Pb} f/C$, during relaxation over longer times.

For the case of o.c.p.–time transients subsequent to a prior cathodic polarization at various s.o.c. values the analysis is more complicated due to the variation of coverage of absorbed hydrogen with potential. However, for the special case of s.o.c. of unity (relaxation from prolonged overcharging) the coverage variations can be neglected and the rate of the $Pb/PbSO_4$ reaction is practically zero compared to the rate of hydrogen evolution. Moreover, mass transfer polarization can be neglected for hydrogen evolution in acid media as limiting currents are very high. In this situation Equation 7 can be approximated as

$$-C(d\eta/dt) + I_{0,H} \exp(-\alpha_H f \eta_H) = 0 \quad (17)$$

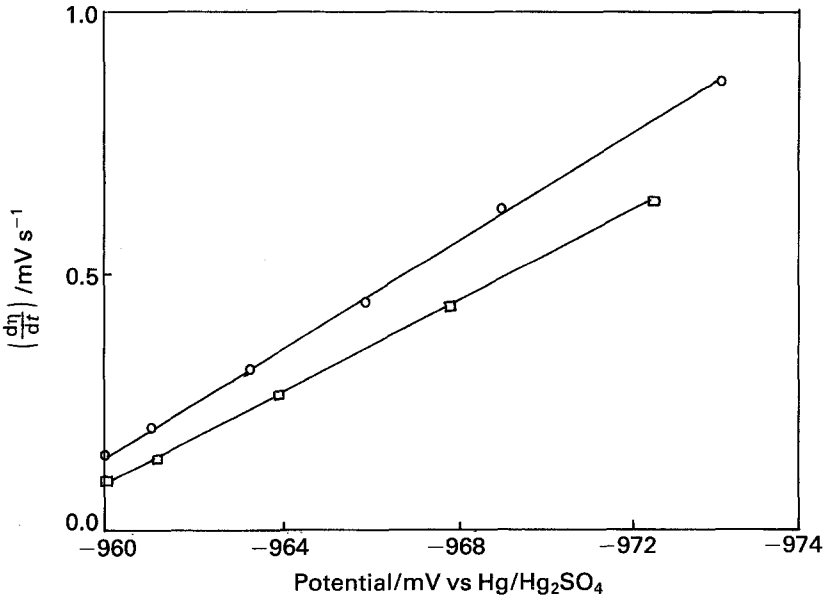

Fig. 6. ($d\eta/dt$) against E plots in gelled electrolyte using the data from Fig. 2 at various s.o.c. values: (○) 0.8 and (□) 0.5.

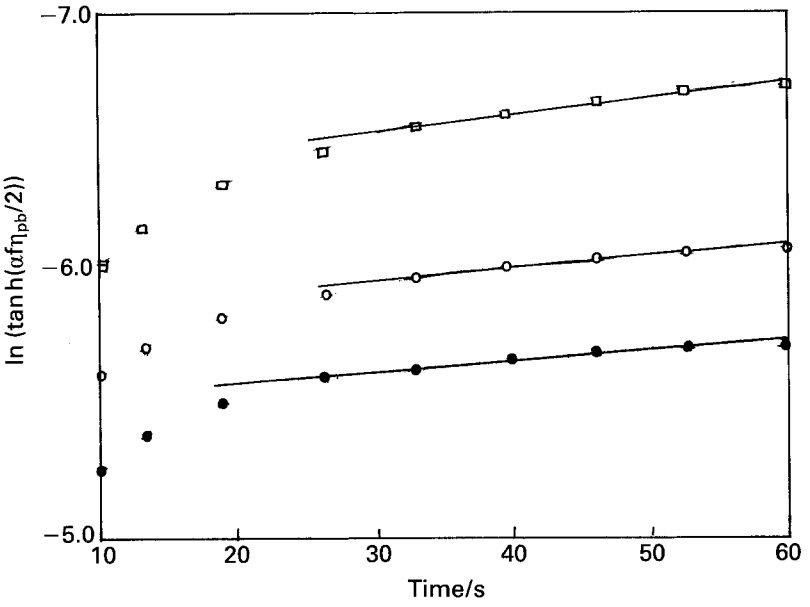

Fig. 7. Ln [tanh ($\alpha f \eta_{Pb}/2$)] against t plots using the data from Fig. 1 at various s.o.c. values: (●) 0.05, (○) 0.2 and (□) 0.5.

Solution of this equation gives

$$\exp(\alpha_H f \eta_H) = (\alpha_H f I_{0,H}/C)t + \text{constant} \qquad (18)$$

Hence a plot of exp ($\alpha_H f \eta_H$) against time should be a straight line with a slope of $(\alpha_H f I_{0,H})/C$, for the special case of s.o.c. equal to unity.

For other s.o.c. values, the cathodic case is similar to that of the anodic and a similar treatment will give a linear relation between $\ln \eta$ and time, whose slope and intercept can be used to calculate the kinetic parameters.

3.2. *Comparison of theory with experimental data*

Figures 5 and 6 show plots of $d\eta/dt$ against E at high s.o.c. values using the data from Figs 1 and 2, respectively. The linearity shown in the case of s.o.c. 0.995 and 0.8 are in good agreement with the analysis expressed in Equation 11. In addition I_{cor}, calculated on the basis of these slopes and apparent geometrical area (with the values of C, α_H and β_{Pb} taken from literature [19]), are 1.5×10^{-7} A cm^{-2} and 0.4×10^{-7} A cm^{-2} for ungelled and gelled electrolyte, respectively. This decrease in corrosion rate is an added advantage in designing maintenance-free batteries using immobilized electrolyte. The deviation from linearity over the larger potential range is more prominent at low s.o.c. values, as the reverse reaction, namely reduction of $PbSO_4$ to Pb, may also contribute; this was neglected during the derivation of Equation 11.

However, at low s.o.c. values Equation 14 must be used and plots of ln [tanh ($\alpha f \eta_{Pb}/2$)] against t are shown in Figs 7 and 8 for free and gelled electrolytes, respectively. The range of linearity is larger for the case of lower s.o.c. values which substantiates the validity of Equation 14. Furthermore, as the slope of these lines are independent of the area of the porous electrode, the variation of slope with s.o.c. can be attributed to the variation of electrochemical reaction rate at different s.o.c. values.

Typical values of $I_{0,Pb}$, calculated on the basis of

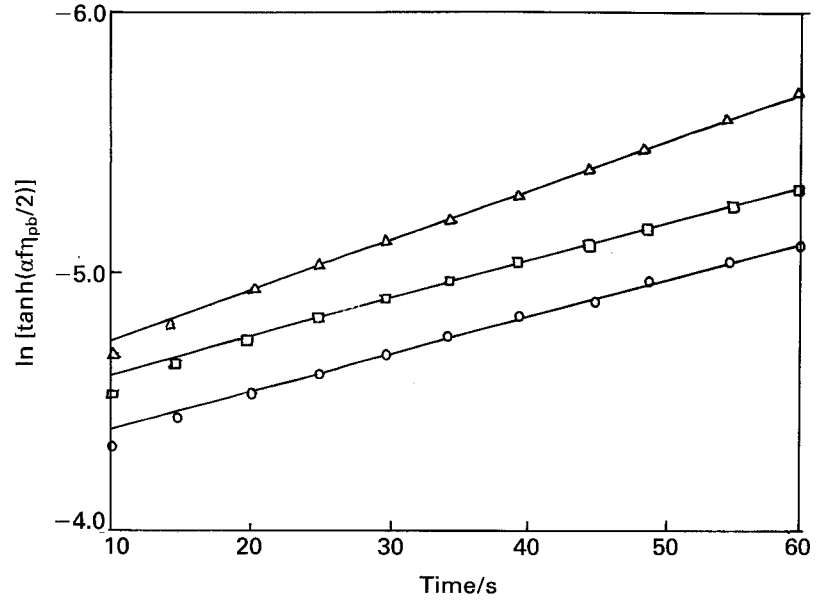

Fig. 8. Ln [tanh ($\alpha f \eta_{Pb}/2$)] against t plots of o.c.p. relaxation from a prior anodic polarization of the Pb/$PbSO_4$ electrode in 4.8 M gelled sulphuric acid using the data from Fig. 2 at various s.o.c. values: (○) 0.05, (□) 0.2 and (△) 0.5.

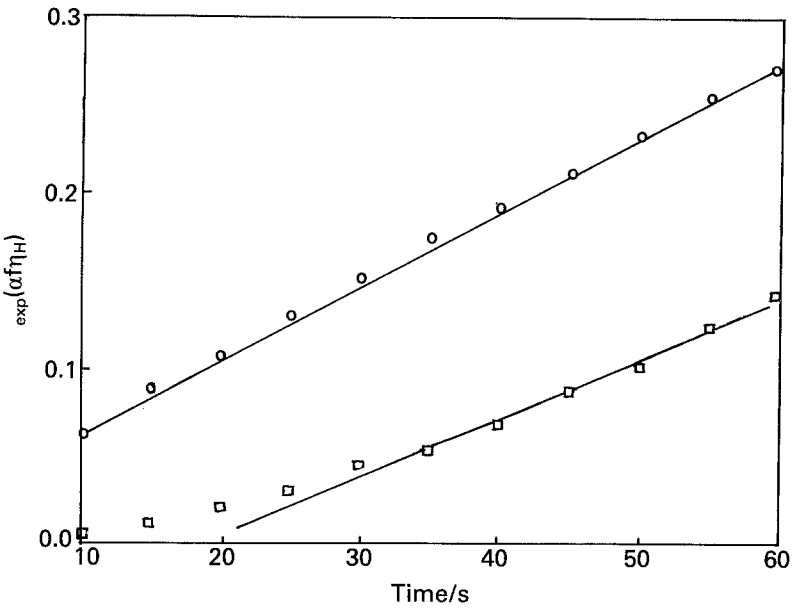

Fig. 9. Exp $(\alpha_H f\eta_H)$ against t plots at unit s.o.c. using the data from Figs 3 and 4; (○) and (□) represent ungelled and gelled electrolyte, respectively.

these plots and the apparent geometrical area (by taking the values of C, α_H and β_{Pb} from the literature [19]) are 5.1×10^{-8} A cm^{-2} and 1.2×10^{-8} A cm^{-2} for ungelled and gelled electrolytes, respectively. Although the magnitude of these values are small in comparison with reported values [14, 19] it is reasonable to expect this on the basis of enhanced actual area due to porosity. This decrease in the exchange current density and extent of linearity change at a particular s.o.c. value can be attributed to the effect of gelling agents like silicate ions on interfacial charge transfer. This, of course, assumes that the double layer capacitance is not changed by the addition of gelling agents, which is not necessarily true. The same conclusions can be obtained by plotting $\ln \eta$ against t as implied by Equation 16.

Figure 9 shows plots of $\exp(\alpha_H f\eta_H)$ against t for o.c.p.–relaxation from a prior cathodic polarization at unit s.o.c. using the data from Figs 3 and 4. The excellent linearity over a large time domain supports the assumptions involved in the treatment. The $I_{0,H}$ values calculated from the slopes are 2.2×10^{-9} A cm^{-2} and 1.5×10^{-9} A cm^{-2} for ungelled and gelled electrolyte, respectively. The slope change due to gelling is insignificant, indicating the absence of any electrocatalytic effects on h.e.r. by sodium silicate.

Plots of $\ln \eta$ against t for o.c.p.–relaxation from a prior cathodic polarization at various s.o.c. values for $Pb/PbSO_4$ electrode in free and gelled electrolyte are shown in Figs 10 and 11, respectively. The large initial deviation from linearity, as predicted by Equation 16, may be attributed to the preference of lead dissolution over hydrogen evolution. The possibility of interference from mass transfer cannot be ruled out completely as Pb^{2+} deposition may occur under diffusion limited conditions, which are not involved in the theoretical analysis. The viscosity effects due to immobilization of the electrolyte may also be important. The extent of deviation is less for the gelled electrolyte as there is increased hindrance for mass transfer especially at lower s.o.c. values. The slope and intercept of these plots can also be used to calculate the kinetic parameters, with a prior

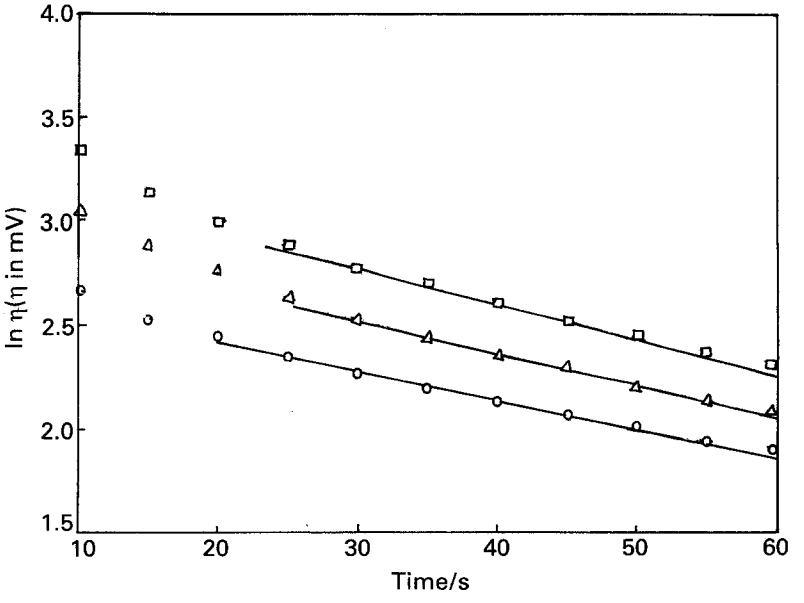

Fig. 10. Ln η against t plots for o.c.p. relaxation from a prior cathodic polarization using the data from Fig. 3 at various s.o.c. values: (□) 0.8, (△) 0.5 and (○) 0.2.

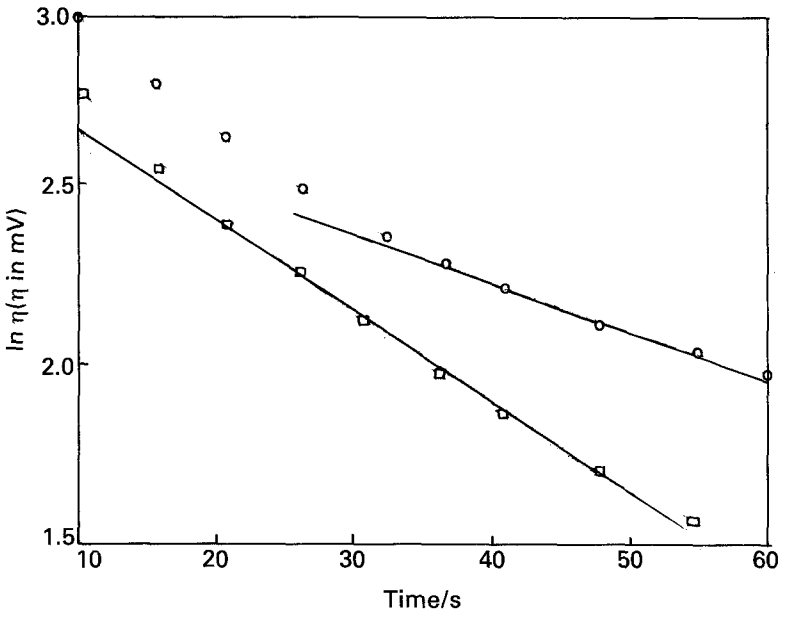

Fig. 11. Ln η against t plots for o.c.p. relaxation using the data from Fig. 4 at various s.o.c. values: (○) 0.5 and (□) 0.2.

knowledge of double layer capacitance and apparent transfer coefficients.

4. Conclusion

A quantitative analysis of o.c.p.–time transients of the $Pb/PbSO_4$ electrode in gelled and non-gelled sulphuric acid shows that there is a substantial change in the self-discharge kinetics of the $Pb/PbSO_4$ electrode as a result of immobilization. This change in the rate of both $Pb/PbSO_4$ and hydrogen electrode reactions will be especially useful in designing maintenance-free lead–acid batteries with gelled electrolytes.

Acknowledgements

The authors acknowledge the late Prof. S. Sathyanarayana of the Indian Institute of Science, Bangalore, for several critical discussions. Financial support from the University Grant Commission (New Delhi) is also acknowledged.

References

[1] G. H. Kelsall, *in* 'Techniques in Electrochemistry, Corrosion and Metal Finishing – a handbook', (edited by A. T. Kuhn), John Wiley, New York (1987) p. 43.
[2] D. A. Harrington and B. E. Conway, *J. Electroanal. Chem.* **221** (1987) 1.
[3] J. A. Butler and J. F. Armstrong, *Trans. Faraday Soc.* **29** (1938) 126.
[4] A. N. Frumkin, *Acta Physiochem., URSS.* **18** (1943) 23.
[5] H. B. Morley and F. E. W. Wetmore, *Can. J. Chem.* **34** (1956) 359.
[6] B. E. Conway and P. L. Bourgault, *ibid.* **37** (1959) 292.
[7] *Idem, Trans. Faraday Soc.* **58** (1962) 593.
[8] P. Ruetschi, *J. Electrochem. Soc.* **120** (1973) 331.
[9] P. L. Bourgault and B. E. Conway, *Can. J. Chem.* **38** (1960) 1557.
[10] B. V. Ratnakumar and S. Sathyanarayana, *J. Power Sources* **12** (1984) 39.
[11] K. Vijayamohanan, A. K. Shukla and S. Sathyanarayana, *ibid.* **21** (1987) 53.
[12] T. P. Driske, *J. Appl. Electrochem.* **1** (1971) 27.
[13] D. Pavlov, *Electrochim. Acta.* **13** (1968) 2051.
[14] J. Sterbe, B. Reichman, B. Mohato and K. R. Bullock, *J. Power Sources* **31** (1990) 43.
[15] R. M. LaFollette and D. N. Bennion, *J. Electrochem. Soc.* **137** (1990) 3693.
[16] K. Vijayamohanan, A. K. Shukla and S. Sathyanarayana, *Electrochim. Acta* **36** (1991) 369.
[17] M. Barek, 'Electrochemical Power Sources', Peter Peregrine, Stevenage (1980) p. 290.
[18] D. Pavlov, *in* 'Power Sources for Electric Vehicle', (edited by B. D. McNicol and D. A. J. Rand), Elsevier, Amsterdam, Oxford (1984) p. 113.
[19] T. F. Sharpe, *in* 'Encyclopedia of Electrochemistry of the Elements', Vol. 1, (edited by A. J. Bard), Marcel Dekker Inc., New York, (1973) p. 308.